Robotics and Autonomous Systems 161 (2023) 104353

Contents lists available at ScienceDirect

Robotics and Autonomous Systems

journal homepage: www.elsevier.com/locate/robot

Human-in-the-loop layered architecture for control of a wearable ankle–foot robot

Uriel Martinez-Hernandez [a,*], Sina Firouzy [b], Pouyan Mehryar [c], Lin Meng [d], Craig Childs [d], Arjan Buis [d], Abbas A. Dehghani-Sanij [b]

[a] Department of Electronic and Electrical Engineering, Faculty of Engineering and Design, University of Bath, Bath, BA2 7AY, UK
[b] School of Mechanical Engineering, University of Leeds, Leeds, LS2 9JT, UK
[c] Healthcare Innovation Centre, School of Health and Life Sciences, Teesside University, Middlesbrough, TS1 3BX, UK
[d] Department of Biomedical Engineering, University of Strathclyde, Glasgow, G1 1XQ, UK

ARTICLE INFO

Article history:
Received 8 September 2020
Received in revised form 7 September 2022
Accepted 27 December 2022
Available online 2 January 2023

Keywords:
Layered architectures
Autonomous systems
Bayesian inference
Sensorimotor control

ABSTRACT

Intelligent wearable robotics is a promising approach for the development of devices that can interact with people and assist them in daily activities. This work presents a novel human-in-the-loop layered architecture to control a wearable robot while interacting with the human body. The proposed control architecture is composed of high-, mid- and low-level computational and control layers, together with wearable sensors, for the control of a wearable ankle–foot robot. The high-level layer uses Bayesian formulation and a competing accumulator model to estimate the human posture during the gait cycle. The mid-level layer implements a Finite State Machine (FSM) to prepare the control parameters for the wearable robot based on the decisions from the high-level layer. The low-level layer is responsible for the precise control of the wearable robot over time using a cascade proportional–integral–derivative (PID) control approach. The human-in-the-loop layered architecture is systematically validated with the control of a 3D printed wearable ankle–foot robot to assist the human foot while walking. The assistance is applied lifting up the human foot when the toe-off event is detected in the walking cycle, and the assistance is removed allowing the human foot to move down and contact the ground when the heel-contact event is detected. Overall, the experiments in offline and real-time modes, undertaken for the validation process, show the potential of the human-in-the-loop layered architecture to develop intelligent wearable robots capable of making decisions and responding fast and accurately based on the interaction with the human body.

1. Introduction

Wearable robots have been developed for decades for the interaction with humans and assistance in applications such as manufacturing, telecontrol, telepresence, healthcare and companion robotics [1–3]. In recent years, wearable robotics has shown rapid progress due to the advances in sensor technology and machine learning, which have allowed the design of lightweight and portable robots with multiple sensors and capable of making decisions [4–6]. Wearable robots have to be able to interact safely with the human body and assist it through accurate decisions and precise control of robot actions. These requirements can be achieved by the development of hierarchical control architectures that allow the robot to sense, make decisions, set control parameters and observe the results of its actions while interacting with the human body.

In this work, a human-in-the-loop layered architecture is presented to allow a wearable ankle–foot robot to sense, make accurate decisions and reliably control its interaction with the human foot during walking activities. Layered architectures have shown their potential for learning and control in areas of robotics such as mobile and bioinspired robotics [7–10], and offer a promising approach for robots that need to interact and assist the human body. The proposed control architecture, composed of high-, mid- and low-level layers, is capable of processing data at different levels of abstraction [11,12]. The high-level layer uses a probabilistic formulation for the recognition of the locomotion activity performed by the human [13,14]. This layer employs angular velocity data from an inertial measurement unit (IMU) attached on the shank of the subject. The mid-level layer uses a finite state machine (FSM) to set the next state and control parameters of the wearable robot during the walking activity. The low-level layer implements a cascade proportional–integral–derivative (PID) control approach for the actual control of the ankle–foot robot attached to the human leg. These layers are synchronised to ensure the

* Corresponding author.
E-mail address: u.martinez@bath.ac.uk (U. Martinez-Hernandez).

https://doi.org/10.1016/j.robot.2022.104353

reliable control of the wearable ankle–foot robot and safe interaction with the human body. The wearable robot, controlled with the proposed human-in-the-loop layered architecture, has been designed using 3D printing technology and an arrangement of DC motors and a capstan wheel to interact with the human foot.

Validation of the human-in-the-loop layered architecture is based on the assistance applied by the wearable robot to the human foot while the subject is walking. This process requires the robot to sense and recognise the walking activity and gait events (toe-off and heel contact) along the gait cycle. These processes employ angular velocity data from an IMU worn by participants on their shank while walking. Then, the output is employed by the wearable ankle–foot robot to assist or lift up the human foot when the toe-off event is detected, and release or move the human foot down when the heel contact event is detected. These experiments are systematically performed in offline and real-time modes. In offline mode, the recognition of walking activity and gait events has shown to be fast and accurate. The real-time mode evaluates the capability of the wearable ankle–foot robot to interact and assist the human foot. This experiment has shown that the robot can control its actions and use feedback from the state of the human body to assist the human foot at the appropriate time while the human is walking. Overall, all the experiments show the capability of the human-in-the-loop layered architecture for control of wearable robots and safely and reliably interact with the human body. Thus, these methods can be used for the development of intelligent and safe systems for interaction and assistance to humans in daily activities. This work substantially extends, with novel software and hardware components and validation processes, our previous work in [15], where a simplified ankle–foot device was developed using rigid metallic materials, one large and heavy DC motor, one PID controller, limited control signals, implemented in an Arduino board, bulky, heavier and less ergonomic.

The rest of this work is organised as follows: the related work on recognition and control methods for wearable robots is presented in Section 2. The proposed control architecture is presented in Section 3. The experiments and results are described in Section 4. The discussion and conclusions are given in Sections 5 and 6, respectively.

2. Related work

In recent years a large variety of wearable robots for interaction and assistance to humans have been developed across the globe. These robots have benefited from the advances in sensor technology, machine learning methods and soft materials [16,17]. Wearable robots, which have been mainly applied in healthcare, manufacturing and telecontrol, need to be capable of controlling its actions through accurate and fast sensing and recognition of human movements [1,18].

Sensing and recognition of human activities have been investigated with different robotic platforms and sensing modalities. Heuristics and six electromyography (EMG) sensors attached on the muscles of participants were used to recognise level-ground walking, ramp ascent and descent activities [19]. Information from floor reaction force, hip and knee joint angles was analysed using a Finite State Machine (FSM) to detect sitting, standing and level-ground walking for control of the HAL-3 robot platform [20]. These methods can recognise activities of daily living (ADLs), but they do not account for the uncertainty in sensor measurements, which make these methods susceptible to fail for small changes in the environment [13]. Computational intelligence offers robust algorithms for perception, decision-making and learning, which are essential for the development of accurate recognition processes in robotics.

Artificial Neural Networks (ANN) and Fuzzy Logic (FL) have been used for the recognition of ADLs such as walking, running, stair ascent and descent with different sensors, e.g., EMG and IMU, and they have achieved accuracies ranging from 88.8% to 99% [21,22]. Accuracies ranging from 99.67% to 99.87% were obtained for the recognition of four locomotion activities combining IMU and pressure sensors [23]. Fusion of ANN and FL improved the identification of multiple ADLs over the use of ANN and FL alone [24]. Support Vector Machines (SVM) with neuromuscular and mechanical sensors were able to recognise walking activities and gait phases with accuracies ranging from 77.3% to 99.0% [25,26]. Probabilistic methods are capable of handling sensor noise and uncertainty in decision-making processes [27]. Examples of these methods include Hidden Markov Models (HMM), Dynamic Bayesian Networks (DBN), Gaussian Mixture Models (GMM) and Gaussian Processes (GP), which are becoming popular for recognition and control in robotics [28,29]. HMMs have been used for the recognition of gait cycle phases (stance and swing) and in-shoe foot pressure sensors [30]. DBN and GP methods, together with wearable sensors, have been able to recognise multiple human activities performed with upper and lower limbs with accuracies ranging from 86.0% to 99.87% [14,31]. GMMs have been used for the recognition of three walking activities with 91.3% to 100% accuracy [32,33].

Wearable robots, together with control methods and multiple sensors, have been used to interact and assist the human body while performing daily activities. Examples of these robot include assistance to sit and stand, grasping and walking on flat surfaces, ramps and stairs. Recognition and assistant to sit, stand and sit-to-stand transition have been investigated with a knee exoskeleton using SVM classifiers, a torque controller and IMUs [34]. Hip assistance has been studied using soft wearable robots composed of textiles, foot-switches, encoders and torque control [35]. A wearable robot and control strategies have been investigated for assistance to posture stability using angle information from the joints and the Wii platform to monitor the Centre of Mass of the wearer [16]. Control of ankle–foot robots has been investigated to assist the human foot based on the state of the body posture during the gait cycle. For instance, control of an ankle–foot robot, built with pneumatic actuators and IMUs, was implemented using the Central Pattern Generator (CPG) approach [36]. Proportional–integral–derivative (PID) controllers were used to control an ankle–foot robot built with soft actuators and encoders [37,38]. A combination of PID methods with encoders and foot switches have been employed for the detection and control of lower limb robots built using soft materials, flat pneumatic actuators and Boden cables [39]. This approach has also been used in the development of upper limb robots and wearable hip robots [40–42]. We employed IMU data, a probabilistic classifier and one PID controller to develop a preliminary and simplified ankle–foot robot in [15]. This device was designed with limited control signals, one large and heavy motor, rigid metallic materials and constrained real-time implementation making it bulky, less ergonomic and limited compared to our current design presented in this paper. All these robots have shown rapid progress using multiple sensors, lightweight materials and advanced methods for recognition and control. Interestingly, most wearable robots still rely on the use of foot switches, potentiometers and heuristic methods for recognition and control processes. Additionally, these robots lack the control architecture for reliable execution of the processes performed at different levels of abstraction (high-, mid- and low-level processes), which are essential in robotic systems for safe interaction with the human body. Thus, the lack of these capabilities makes these robots susceptible to failure to even slight changes in the environment.

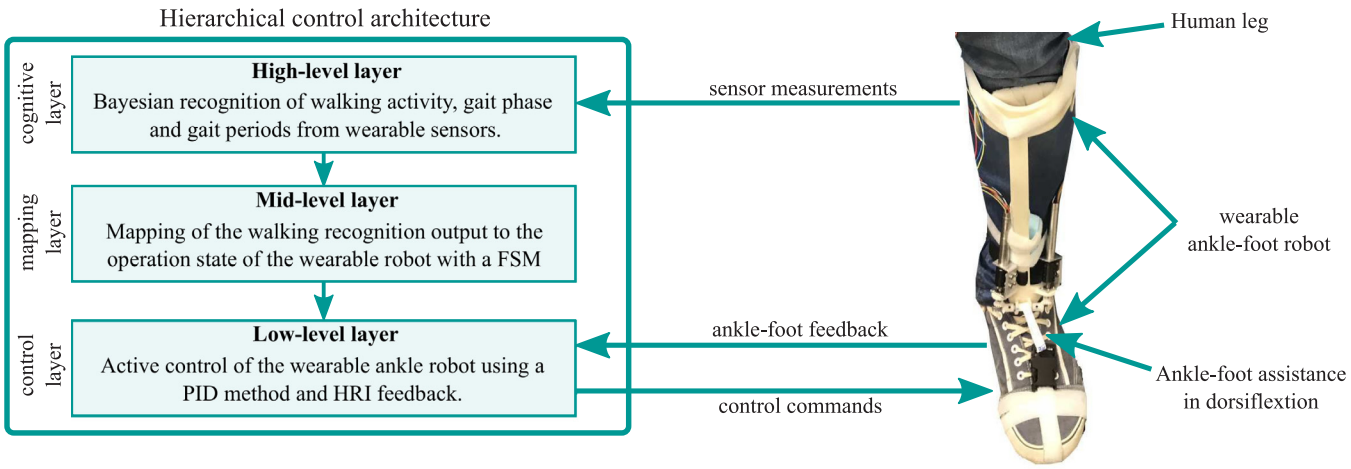

Fig. 1. Human-in-the-loop layered architecture for control of a wearable ankle–foot robot.

(A) Level-ground walking (B) Ramp ascent (C) Ramp descent

Fig. 2. Data collection using an IMU from three walking activities. (A) level-ground walking, (B) ramp ascent and (C) ramp descent.

In this research work, a human-in-the-loop layered architecture is proposed for the control of a wearable ankle–foot robot while interacting with the human body. This layered architecture allows the wearable robot to sense, make decisions, set the control parameters and control its actions using a set of high-, mid-, and low-level layers precisely synchronised. This approach is implemented in a wearable ankle–foot robot developed using 3D printing technology, soft components and miniature actuators, to assist the human foot during walking activities. The wearable robot provides reliable assistance to the human foot (lift the foot up) when the toe-off event is detected during the gait cycle. When the heel contact event is detected, no assistance is required and the robot allows the human foot to move freely without interfering with the natural foot movement. The sensor modules, computational and control methods, and the wearable ankle–foot robot are described in Section 3.

3. Methods

The proposed human-in-the-loop layered architecture for control of a wearable ankle–foot robot is composed of high-, mid- and low-level layers. These layers process data from an IMU module to detect walking and gait events, set the control signals and control the ankle–foot robot to interact with the foot of the subject while walking (Fig. 1).

3.1. Data collection and processing

Twelve healthy male subjects were recruited from the School of Mechanical Engineering at the University of Leeds, to collect data for training and testing the methods presented in this work. The subjects were free from gait abnormalities; their ages ranged between 24 and 34 years old, heights between 1.74 m and 1.79 m, and weights between 77.6 kg and 85 kg.

Angular velocity signals were collected from a 9-DoF IMU attached to the lower leg of participants (Fig. 2). Sensor signals were sent wirelessly to a central computer. Piezoresistive insole sensors were used to detect the beginning of the gait cycle as part of the data collection. Participants walked at their self-selected speed with ten repetitions of three walking activities; level-ground walking, ramp ascent and descent. For level-ground walking, a flat surface was employed, while a metallic ramp with an 8.5 deg slope was used for ramp ascent/descent as shown in Fig. 2. Angular velocity signals were collected at a sampling rate of 100 Hz, and stored for training and testing the methods for recognition of walking activity and gait periods to control the assistive robot as described in Section 3.3.

The measurements from the three walking activities are shown in Fig. 3(a). Mean angular velocities and standard deviations are shown by solid and dashed lines, respectively. Angular velocities from each gait cycle were used to construct the histograms required for the recognition method. In this work, the gait cycle was divided into stance phase (initial contact, loading response, mid stance, terminal stance, pre-swing) and swing phase (initial swing, mid swing and terminal swing). Fig. 3(b) shows an example of the constructed histograms for the recognition of walking and gait periods.

3.2. Wearable ankle–foot robot

A wearable ankle–foot robot is built to validate the human-in-the-loop layered architecture. The Computer-Aided Drawing (CAD) model and real wearable robot are shown in Fig. 4. The device has been designed and developed to fit the lower leg using 3D printing technology (Object1000 from Stratasys Inc). The ergonomic design and construction makes this device lightweight, comfortable and durable.

Two Maxon ECX brushless DC (BLDC) motors are mounted on the wearable device and combined with a gearbox with a ratio of 25:1. The nominal torque output from each gearbox is 76 mNm, applied at speeds up to 800 rpm to lift up the human foot while walking. The gearbox shafts, connected to an arrangement of bevel gears, transfer the motion to a horizontal rigid shaft. The shaft performs as a capstan connected to a strap (tendon), which is connected to the wearer's shoe by a buckle. The rotation of the capstan winds in the strap to pull the user's foot upwards during the assistance mode. The capstan unwinds the strap allowing the robot to move down the wearer's foot during the release mode. For synchronised communication and control of the BLDC motors, two motor drivers ESCON 50/54 and an FPGA-based myRIO board

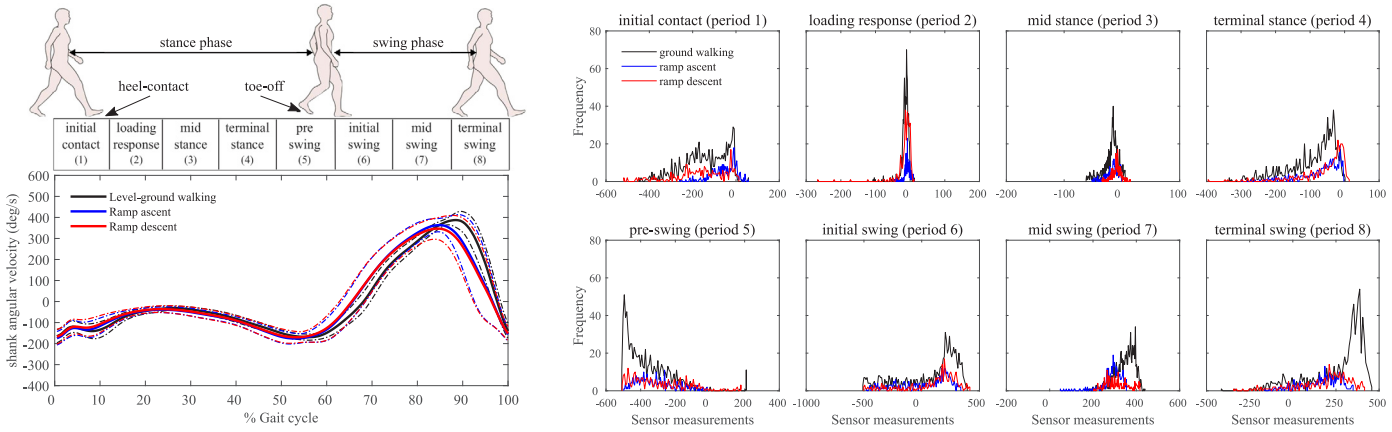

(A) Angular velocity signals from walking activities

(B) Gait periods that compose the walking cycle

Fig. 3. Angular velocity from level-ground walking, ramp ascent and descent walking activities. Solid and dashed-lines show the mean and standard deviation. (A) Gait cycle segmented into eight periods, which are processed to know the state of the human body during the gait cycle. (B) Histograms for recognition of walking and gait phase. The gait periods composed the stance (period 1 to period 5) and swing (period 6 to period 8) phases of the gait cycle.

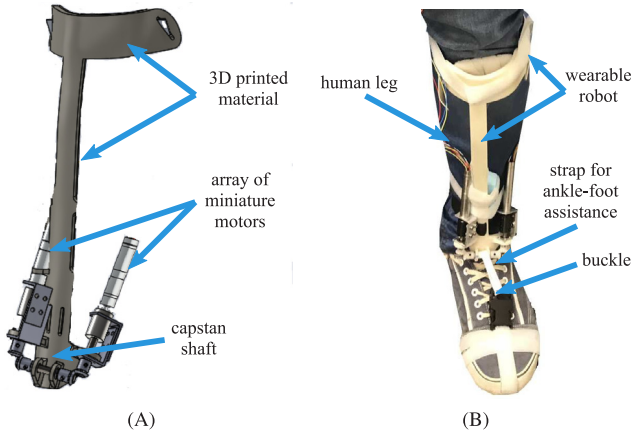

Fig. 4. 3D printed wearable ankle–foot robot composed of miniature DC motors, capstan shaft and bevel gears. (A) CAD model of the assistive device and (B) real wearable robot attached on the human leg.

are employed. The motor drivers perform proportional–integral (PI) current control, and provide feedback on the state of the motor including current (and therefore, torque) and speed. The myRIO board is employed for synchronised and real-time control of both motors via a PID speed control algorithm as explained in Section 3.5. The lightweight and ergonomic structure, materials and actuation approach, and real-time implementation and control using an FPGA board for this wearable device are improvements over the preliminary design of our previous work in [15].

3.3. High-level recognition of walking and gait periods

A Bayesian approach together with a competing accumulators approach is developed for the high-level layer to recognise the walking activity and gait periods. The approach updates the posterior probability from the product of the prior and likelihood. Sensor measurements and perceptual classes are represented by z and $c_n \in C$, respectively. Each perceptual class c_n is defined by a (u_k, v_l) pair, where u_k with $k = 1, 2, \ldots, K$ and v_l with $l = 1, 2, \ldots, L$ are the walking activities and gait periods. The Bayesian approach is as follows:

$$P(c_n|z_t) = \frac{P(z_t|c_n)P(c_n|z_{t-1})}{P(z_t|z_{t-1})} \tag{1}$$

where $P(c_n|z_t)$ and $P(z_t|c_n)$ are the posterior probability and likelihood at time t. The prior probability at $t-1$ is $P(c_n|z_{t-1})$. The variable u_k with $K = 3$ are the three walking activities, while v_l with $L = 8$ are the eight gait periods used for recognition. The gait periods can be used to determine when the human is on the stance and swing phases. The prior probability is uniformly distributed at time $t = 0$, $P(c_n) = P(c_n|z_0) = \frac{1}{N}$, where z_0 are sensor measurements and N is the number of (u_k, v_l) pairs. For time $t > 0$, the prior probability is updated by the posterior probability estimated at $t-1$.

Angular velocities are obtained at each time step from the IMU, $S_{\text{sensors}} = 1$, attached to the lower leg of participants. Histograms from IMU data, (Fig. 3B), are used for the construction of the measurement model for the Bayesian method. This model is used to estimate the likelihood of a perceptual class, c_n, given an observation z_t, as follows:

$$P_s(b|c_n) = \frac{h_{s,n}(b)}{\sum_{b=1}^{N_{\text{bins}}} h(b)} \tag{2}$$

where $h_{s,n}(b)$ is the sample count in bin b for sensor s over all training data in class c_n. The model bins angular velocity signals into $N_{\text{bins}} = 100$ intervals. The values are normalised to have probabilities in [0, 1]. Eq. (2) estimates the likelihood of observation z_t over all sensors, as follows:

$$\log P(z_t|c_n) = \sum_{s=1}^{S_{\text{sensors}}} \frac{\log P_s(w_s|c_n)}{S_{\text{sensors}}} \tag{3}$$

where w_s is the sample from sensor s and $P(z_t|c_n)$ is the likelihood of z_t, given a class c_n. Normalised values are ensured with the marginal probabilities conditioned on previous sensor observations as follows:

$$P(z_t|z_{t-1}) = \sum_{n=1}^{N} P(z_t|c_n)P(c_n|z_{t-1}) \tag{4}$$

The posteriors, (u_k, v_l), are the joint distributions of the walking activities, u_k, and gait periods, v_l. The beliefs over individual walking activity and gait period classes are given by the marginal posteriors, as follows:

$$P(u_k|z_t) = \sum_{l=1}^{L} P(u_k, v_l|z_t),\ P(v_l|z_t) = \sum_{k=1}^{K} P(u_k, v_l|z_t) \tag{5}$$

The Bayesian process implements a competing accumulator approach to make decisions. The Bayesian update process stops

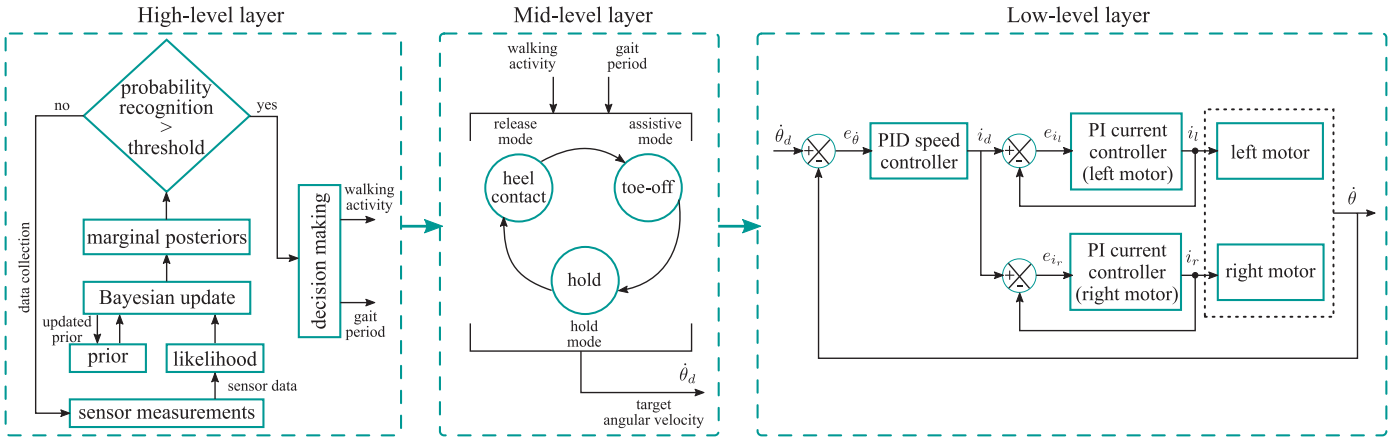

Fig. 5. Human-in-the-loop layered architecture for control of a wearable ankle–foot robot. The high-level layer uses a Bayesian approach together with a competing accumulator method for the recognition of walking. The mid-level layer uses an FSM to prepare the control parameters of the wearable robot. The low-level layer is responsible for delivering the actual control of the wearable robot using a cascade PID control approach.

once the belief accumulated by one of the classes exceeds the belief threshold β, which can be set to a value in the range of 0.0 and 0.99. Then, a decision is made with the *maximum a posteriori* (MAP), to estimate the walking activity and gait period classes, as follows:

$$\text{if any } P(u_k, v_l|z_t) > \beta \text{ then}$$
$$\hat{u}_k = \arg\max_{u_k} P(u_k|z_t), \qquad \hat{v}_l = \arg\max_{v_l} P(v_l|z_t) \tag{6}$$

where $\hat{v}_k$ and $\hat{v}_l$ are the estimated walking activity and gait period pair. The parameter β is iteratively updated with values from 0.0 to 0.99 and increments of 0.01 to analyse their effect on the adjustment of the recognition accuracy and speed at same time. The Bayesian process is implemented in the high-level layer of the hierarchical architecture as shown in Fig. 5.

3.4. Mid-level layer control for synchronisation

The walking activity and gait period estimated from the high-level layer are used by the mid-level layer to determine whether the wearable robot needs to be in 'assistive', 'hold' or 'release' mode (Fig. 5). The transition between the 'assistive', 'hold' and 'release' modes of the wearable robot is controlled by the 'toe-off', 'hold' and 'heel contact' states in a FSM, respectively. In each state, the control parameters are prepared for controlling the ankle–foot wearable robot.

The output from the mid-level layer, fed into the low-level layer, takes one of three values: -1, 0 and 1, which correspond to 'heel contact', 'hold' and 'toe-off' states, respectively. The desired motors' speed, which is employed by the low-level layer, is calculated by multiplying the mid-level output by a fixed value obtained as explained in Section 3.5. The motor speed can be zero, positive or negative when the mid-level layer outputs 0, 1 or -1, respectively. These signals and the low-level layer, described in Section 3.5, control the motor actions of the wearable robot to assist (lift up) the human foot at the appropriate time. The mid-level layer also sends the target angular velocity to control the motors of the wearable device. All these signals are required to ensure that the wearable ankle–foot robot reliably interacts and assists the human foot.

When the toe-off event is recognised by the high-level layer, the FSM enters the 'toe-off' state, and sends a positive speed command to the low-level controller. This causes the human foot to be lifted up ('assistive' mode) by the wearable robot until the target position is reached. Then, the FSM enters the 'hold' state, and the motors' speed becomes zero, holding the human foot ('hold' mode) at the target position. Once the high-level layer predicts the heel-contact event, the mid-layer enters the 'heel contact' state, and sends a negative speed signal to the low-level layer. This causes a downward movement of the human foot ('release' mode) until the target loose position is reached. Then, the FSM enters the 'hold' state and the whole process is repeated continuously during the walking cycle.

The state machine does not simply follow a predefined procedure, but makes decisions based on the recognition from the high-level layer and the current state of the wearable robot. This means that if the current robot state is 'release' mode (the foot is allowed to move downwards), and the high-level layer detects the toe-off event before the loose position is reached, then the mid-level layer immediately enters the 'toe-off' state to assist the human foot. Similarly, if the mid-level layer is in the 'assistive' state (lifting the foot up) and the heel contact event is detected before reaching the target position, then mid-level layer immediately enters the 'heel contact' state to release the human foot. This approach allows compliance of the mid-level layer according to the signals from both sources, the high-level layer and the state of the wearable robot.

3.5. Low-level layer for robot control

The low-level controller, responsible for the control of the wearable ankle–foot robot (see Section 3.2 and Fig. 4), uses a cascade PID controller (Fig. 5). This approach tracks the motors' target speed signal sent by the mid-level layer. The motors' target velocity value, $\dot{\theta}_d$, required for the 'assistive' and 'release' modes, was determined by iterative tuning analysis of the control system until a stable response was achieved. This cascade PID approach, used to control both the speed and current of the array of mini BLDC motors, is a novel and improved component over the single PID position control implemented in our previous preliminary work in [15].

The velocity error, $e_{\dot{\theta}}$, is computed by subtracting the actual velocity, $\dot{\theta}$, from the desired velocity $\dot{\theta}_d$. The velocity error is fed into the outer loop (Fig. 5), which is a PID speed controller that creates the desired current value, i_d, for the left and right motors of the wearable ankle–foot device. The i_d value is fed into the two inner loops, composed of PI current controllers, each for one of the motors. Sending the same target current command simultaneously to both motors, ensures that they contribute equally to the actuation effort during assistance to the human foot. The equal contribution of both motors avoids the unbalanced actuation and overheating that can be presented if

one of the motors applies a larger effort than the other one. Both motors provide current feedback, i_l and i_r, which together with the current errors, e_{i_l} and e_{i_r}, are fed into the PI current controllers. The two PI current controllers are independent, while a single PID speed controller is used for both motors. This cascade control approach is suitable because the shafts of the motors are connected to each other, and therefore, they rotate at the same angular velocity. The equations describing the low-level control algorithm are as follows:

$$e_{\dot{\theta}} = \dot{\theta}_d - \dot{\theta} \tag{7}$$

$$i_d = K_p\, e_{\dot{\theta}} + K_i \left(\int_0^t e_{\dot{\theta}}\, dt \right) + K_d \frac{de_{\dot{\theta}}}{dt} \tag{8}$$

The velocity error is defined by $e_{\dot{\theta}}$, while K_p, K_i and K_d are the coefficients of the PID controller. The PI and PID coefficients were tuned prior to using the wearable robot. The PI coefficients were tuned with an automatic algorithm provided by the motor control manufacturer. The PID controller was tuned using a systematic iterative tuning process instead of classical tuning methods like Ziegler/Nichols, which require periodic input commands that could be harmful for the subject while interacting with the wearable ankle–foot robot. The integral and derivative coefficients were initially set to zero, and the proportional coefficient (Eq. (8)) was determined with the device operating without any load. Next, the proportional coefficient was gradually increased until signs of instability were observed. The largest stable value was chosen for the proportional gain. A similar iterative approach was used for the integral gain with several iterations performed slightly increasing the derivative gain to find the largest stable value. Then, K_p and K_i were increased as the existence of the action from the K_d coefficient allows for larger proportional and integral gains without causing instability. This process provided a set of coefficients for fast and stable response.

The high-, mid- and low-level layers have been implemented into a hierarchical architecture (Figs. 1 and 5) in order to synchronise all the processes and ensure a reliable and accurate control of the wearable robot. This aspect is important given that the robot physically interacts and assist the human body. This layered architecture is described in Section 3.6.

3.6. Hierarchical layered architecture for robot control

All the methods used by the high-, mid- and low-level layers are implemented in the layered architecture (Figs. 1 and 5). This hierarchical layered architecture allows the synchronisation and communication of the processing modules required for the robust control of the wearable ankle–foot robot. The sensor data from the IMU module is received and processed by the high-level layer. This layer estimates the walking activity and gait period with the Bayesian perception approach. These results are sent to the mid-level layer, which using the FSM, sets the next robot state and target motor speed signals to the low-level controller. Then, the target speed is tracked by the low-level layer, using PID and PI controllers in a cascade control configuration, for the delivery of the actual control of the wearable ankle–foot robot while the human walks.

The wearable ankle–foot robot moves to the ‘assistive’ mode (lift up the human foot) when the toe-off event is detected by the high-level layer while the human is walking. The assistance is deactivated and the robot moves to the ‘release’ mode (the foot moves downwards) when the recognition method detects the heel contact event. The low-level controller also uses motor position feedback while the human walks to avoid pulling the user’s foot too far upward, and thus, ensuring a safe performance at all times of the wearable ankle–foot robot.

4. Results

This section describes the three experiments performed and the results obtained with the human-in-the-loop layered architecture and wearable ankle–foot robot. First, the recognition of walking, gait periods and gait events was performed using data from an IMU. Second, the control of the robot was tested with a subject wearing the ankle–foot robot, using sensor data from an IMU attached on the leg of another subject performing a walking activity. Third, the control of the wearable robot was tested with a subject wearing both the ankle–foot robot and IMU sensor while performing a walking activity.

4.1. Recognition of walking activity

First, the accuracy for recognition of walking with the probabilistic approach is evaluated. For the training and testing phases of the recognition method, IMU data was collected from participants while walking (see Figs. 2 and 3).

The decision threshold β, with iterative increment steps of 0.01, was employed to control the Bayesian updating process and adjust at the same time both the recognition accuracy and speed of walking activities, as shown in Fig. 6. The plots show the mean results obtained by performing 10,000 iterations or decisions for each increment value in the decision threshold. The recognition of walking activity shows mean errors of 21% (79% accuracy) and 0.13% (99.87% accuracy) for decision thresholds $\beta = 0.0$ and $\beta = 0.99$, respectively (Fig. 6A). These recognition accuracies were achieved with a mean of 1 and 24 sensor samples for $\beta = 0.0$ and $\beta = 0.99$ (Fig. 6B). Thus, the high-level layer needed a mean of 24 data samples to estimate the walking activity with 99.87% accuracy. This analysis is important given that robots need to make accurate decisions but also to respond in the appropriate time.

Recognition of stance and swing phases was analysed to estimate the state of the human body while walking. This analysis used data from the eight gait periods of the gait cycle, where stance phase is composed of gait periods 1 to 5 (initial contact, loading response, mid stance, terminal stance, pre-swing) and swing phase of gait periods 6 to 8 (initial swing, mid swing, terminal swing), respectively (Fig. 3(a)). The recognition achieved mean errors of 7% (93% accuracy) and 0.8% (99.20% accuracy) for $\beta = 0.0$ and $\beta = 0.99$, respectively (Fig. 6A). A mean of 13 data samples were needed for recognition of gait periods with accuracy of 99.20% (Fig. 6B).

The confusion matrices in Fig. 6C,D show the recognition of each walking activity, gait period and gait phase. Level ground-walking, ramp ascent and descent were recognised with 100%, 100% and 99.60% accuracy, respectively. Gait periods 1 to 8 achieved 99.1%, 100%, 99.4%, 100%, 99.9%, 98.3%, 98.9% and 98.3% accuracy, respectively. Stance and swing phases were recognised with 99.68% (mean of periods 1 to 5) and 98.5% (mean of periods 6 to 8) accuracy. Gait phase recognition was also evaluated in real-time with subjects walking on a treadmill and a motion capture system. The subjects walked at their comfortable speeds for approximately 1 min, while wearing an IMU on their shanks. The estimation of stance and swing phases was validated with a 12 camera VICON motion capture system (Vicon MX Giganet, Oxford Metrics Ltd., UK) using reflective markers on the lower limb segments [49]. The mean recognition accuracies from both, the high-level recognition and the motion capture system, were 95.78% and 95.71% for the stance and swing phase, respectively. Other works have also shown accurate recognition of locomotion activities using a variety of wearable sensors including EMGs, IMUs, goniometers and foot switches, and computational methods such as DBN, LSTM, SVM, LDA with recognition accuracy

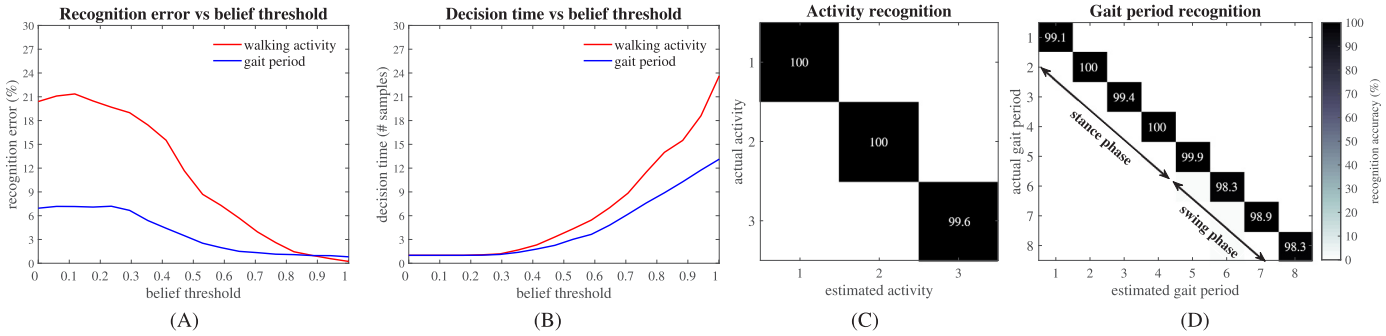

Fig. 6. Recognition of walking activities and gait periods. (A) Mean recognition error of 0.13% and 0.8% for walking activity and gait period, respectively. (B) Mean decision time of 24 and 13 data samples for the highest recognition accuracy of walking activity and gait period, respectively, with $\beta = 0.99$. (C) Recognition accuracy of individual walking activities: (1) level-ground walking, (2) ramp ascent, (3) ramp descent. (D) Recognition accuracy of gait periods with (1) initial contact, (2) loading response, (3) mid stance, (4) terminal stance, (5) pre-swing, (6) initial swing, (7) mid swing and (8) terminal swing, and stance and swing phases.

Table 1
Comparison of state-of-the-art computational methods for recognition of walking activities and recognition of gait periods.

Method	Activity	# Sensors	Sensor type	Activity recognition		Gait period recognition	
				Accuracy (%)	Decision time (ms)	Accuracy (%)	Decision time (ms)
SVM [25]	LGW, RA RD, Stairs	9	EMG, load cell	99	150	97	–
DBN [31]	LGW, RA LD, Stairs	13	IMU, load cell	98	300	95.25	–
LDA + DBN [43]	LGW, RA RD, Stairs	13	IMU, load cell goniometer	99.5	300	–	–
GMM [32]	LGW Standing Sitting	4	IMU, load cells goniometers	100	100	–	–
Ensemble [5]	LGW, RA RD, Stairs	9	IMU	97.60	–	–	–
Bayesian LDA [44]	LGW, RA RD, SD, SA	4	sEMG, position force	96.10	–	99.20	–
ANN [45]	LGW	5	IMU, pressure foot insoles	–	–	95.24	–
kNN [46]	LGW	5	pressure foot insoles	–	–	81.43	–
LSTM [47]	LGW, RA, RD SA, SD, Stop	5	IMU	96.10	–	–	–
CNN + LSTM [48]	LGW, RA, RD SA, Sitting	3	IMU	96.37	–	–	–
Our approach	LGW, RA RD	1	IMU	99.87	240	99.20	130

ranging from 93% to 100% and decision time from 150 ms to 300 ms, as shown in Table 1. However, only a few works, including our proposed method, have investigated approaches for the recognition of both walking activity and gait periods achieving walking accuracies between 96.10% and 99.87% and gait period accuracies between 81.43% and 99.20%.

4.2. Response of the wearable robot with human-in-the-loop

The control and response of the wearable robot was validated with a Human-in-the-Loop approach implemented in two scenarios. In the first scenario, a subject was wearing an IMU module on his lower limb while walking at his self-selected speed to read sensor data and perform the walking recognition process. A second subject was wearing the ankle–foot robot while sitting on a stool, with his foot relaxed, to get his foot lifted up or assisted by the wearable robot (Fig. 7A). This experiment allowed the analysis of the capability of the human-in-the-loop layered architecture to control the wearable robot in a static mode (no walking). The layered architecture recognises the walking activity (high-level layer) performed by the subject wearing the IMU module. In this experiment, the decision threshold of $\beta = 0.99$ was selected to achieve high recognition accuracy according to the results obtained from the analysis in Section 4.1. The output signal is used to set the control parameters and next state (mid-level layer) of the robot. The information is used by the low-level layer to send the control signals in order to lift up (assist) or move downwards (release) the foot of the subject wearing the ankle–foot robot. The system response in Fig. 7B shows the signal sent by the mid-level layer, normalised motor angle feedback and output assistive power, represented by blue, orange and green colours, respectively. These signals were obtained while the subject wearing the IMU module was walking. The signals from the mid-level layer are -1, 0 and 1, which represent the 'release', 'hold' and 'assistive' states of the wearable robot, respectively. These signals prepare the robot to lift up (assist) and move downwards (release) the human foot when the toe-off and heel contact events are recognised, respectively. The robot keeps the foot up at certain position ('hold') before the heel contact event is detected and move to the release state.

The command signal shows the recognition of heel contact and toe-off from the subject wearing the IMU module. The output power was calculated by multiplying the motors' current by their

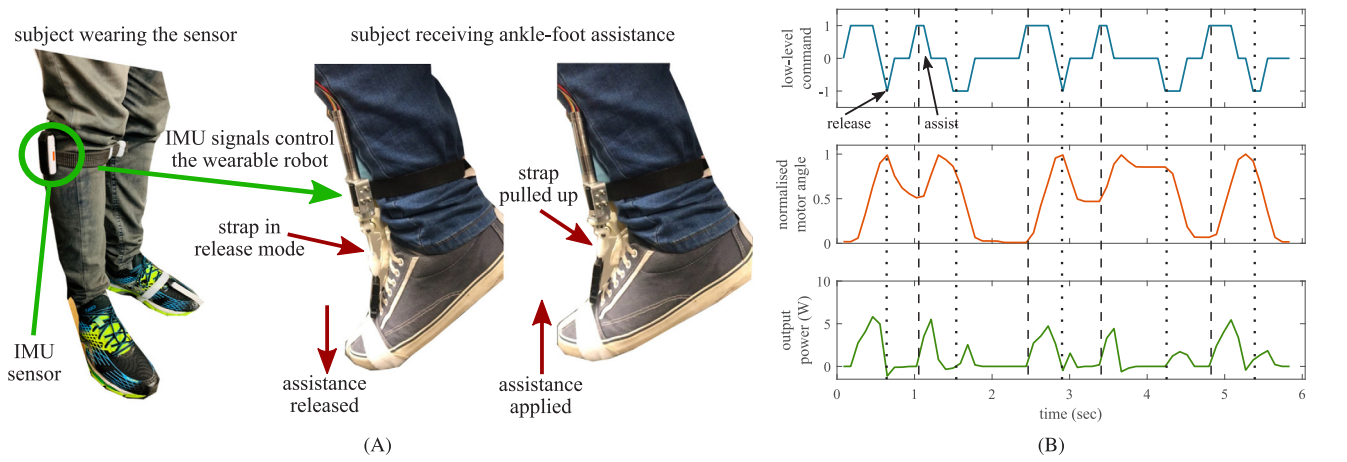

Fig. 7. Validation of the human-in-the-loop layered architecture for control of a wearable ankle–foot robot. Scenario 1, a subject wears the ankle–foot robot and another subject wears the IMU module while walking. (A) The subject on the left wears the IMU while walking. The subject on the right wears the ankle–foot robot, while sitting on a chair for real-time assistance. (B) Output signals from the experiment with the wearable robot. (top) Command sent to control the wearable robot. The dotted- and dashed-lines show the release and assistance applied to the human foot when the heel contact and toe-off events are detected. (middle) Normalised motor angle feedback from the wearable robot. (bottom) Output power from the wearable robot for assistance to the human foot. (For interpretation of the references to colour in this figure legend, the reader is referred to the web version of this article.)

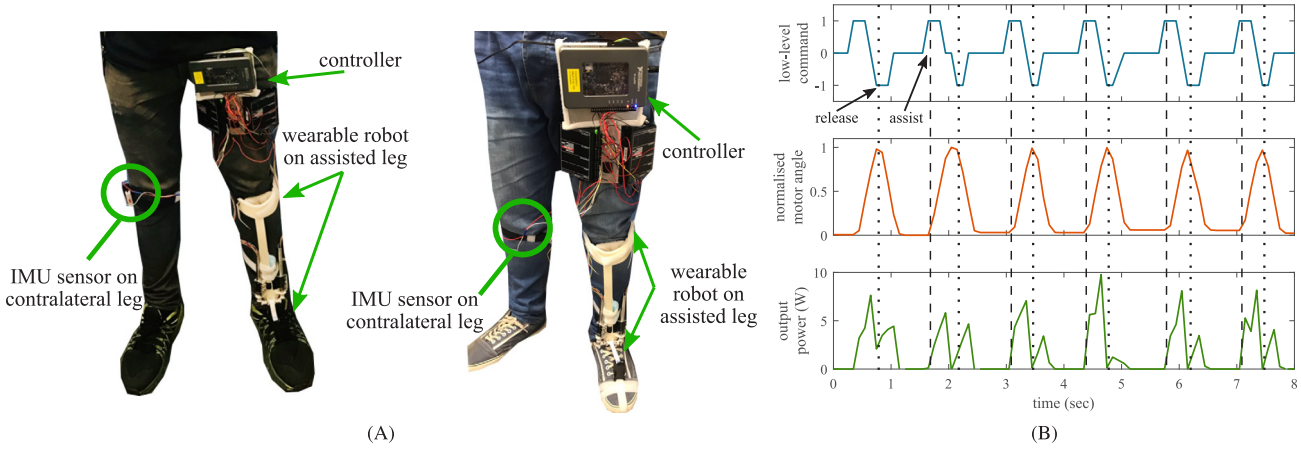

Fig. 8. Validation of the human-in-the-loop layered architecture for control of a wearable ankle–foot robot. Scenario 2, a subject wears both the ankle–foot robot and the IMU module while walking. (A) The participants walked at their self-selected speed while wearing the robot and sensor. (B) Output signals from the experiment with the wearable robot. (top) Command sent to control the wearable robot. The dotted- and dashed-lines show the release and assistance applied to the human foot when the heel contact and toe-off events are detected, respectively, by the high-level layer. (middle) Normalised motor angle feedback from the wearable robot. (bottom) Output power from the wearable robot for assistance to the human foot.

torque constant, and multiplying the result by their angular velocity. An efficiency factor of 85% for the gearing mechanism was used in the calculation (based on the manufacturer's datasheet). The output power increases when the foot is lifted up or assisted by wearable ankle–foot robot (Fig. 7B). The assistance is represented by the large output power peak that follows the 'assist' low-level command and normalised motor angle value of 1 corresponding to the user's foot in the target upper position. A low output power peak follows the 'release' low-level command representing the wearable robot moving the user's foot to the target loose position. This low output power is required to break the inertia and friction of the motors.

In the second scenario for the evaluation of the human-in-the-loop layered architecture, a subject was asked to attach the wearable sensor on his lower limb and put on the wearable ankle–foot robot (Fig. 8A). This experiment allowed the analysis of the capability of the complete system to lift up (assist) and move downwards (release) the human foot when the toe-off and heel contact events are detected while walking.

The subject wore the ankle–foot robot on one leg and the IMU on the contralateral leg. The subject was asked to walk at his self-selected speed, relax his muscles and avoid lifting up his foot during the toe-off or swing phase of the gait cycle. This experiment permitted the observation of the robot response in terms of the output power and position feedback while lifting up (assist) and moving downwards (release) the human foot. Fig. 8B shows the command signal, normalised motor angle feedback and output power of the wearable robot.

When the tow-off event was detected, the wearable robot entered the 'assistive' mode lifting up the human foot to a target upper position. The assistance power used by the robot and the normalised motor angle feedback increased while lifting up the foot. Once the foot is at the target upper position, there was a short period of time where the foot was steady ('hold' mode) before moving the foot downwards to the target loose position. When the heel contact was detected, the robot entered to the 'release' mode, allowing the user's foot to move downwards to a loose position. Similar to the previous experiment, in the 'release'

mode a low output power was required to overcome the inertia and friction of the motors and gears. This power was lower than the one needed for lifting up the foot. The normalised motor angle also decreased while moving downwards the human foot to allow it to contact the floor.

5. Discussion

In this research, a human-in-the-loop layered architecture for a wearable ankle–foot robot control was presented as a proof-of-concept for interaction and assistance to the human body. The control architecture was composed of high-, mid- and low-level layers. Layered architectures allow the development of devices capable of learning and safely interacting with the human body and the environment [7,50].

The high-level layer implemented a Bayesian formulation, together with a competing accumulator approach, to make decisions and estimate the walking activity, gait period and gait phase performed by the human. This processing layer employed data from an IMU sensor attached on the shank of the subject. This recognition process showed to be capable of making accurate and fast decisions by adjusting a decision threshold manually. High accurate decisions required a large number of samples compared to low accurate decisions, which is expected given that the systems needs more sensor data or evidence to reduce the uncertainty of its decision. This trade-off between speed and accuracy, commonly observed in decision making systems, can be set according to the application requirements by selecting the decision threshold value to be employed by the competing accumulative approach. In this work, the decision threshold was set manually, however, we plan to investigate approaches to make this parameter capable of adapting autonomously over time to achieve specific requirements, as part of our future work. The proposed recognition method is capable of recognising walking activity, gait periods and phases, which is an enhanced feature compared to other state-of-the-art methods that recognise only walking activity [31,48]. Our method was able to achieve high recognition accuracy using 1 wearable sensor compared to other advanced methods that required between 5 and 13 sensors to achieve similar accuracy [5,44,47].

The mid-level layer implemented an FSM to set the next robot control mode ('hold', 'assistive', 'release') triggered by the detection signal from the high-level layer. This process prepared the parameters to control the wearable robot. These control parameters were employed by the lower-level layer, which was implemented with a cascade PID control approach for the precise control of the wearable ankle–foot robot.

The human-in-the-loop layered architecture was tested using a wearable ankle–foot, which was developed to lift up and move downwards the human foot when the toe-off and heel contact events are detected during the walking cycle. The wearable ankle–foot robot was designed and fabricated using lightweight and soft materials with 3D printing technology. The robot actuation system used an arrangement of miniature motors, bevel gears and capstan shaft, which contrasts with previous systems built with large and heavy motors, and pneumatic actuators [51,52]. A strap, attachable to any foot size allowed the robot to lift up (assist) and move downwards (release) the human foot. The wearable ankle–foot robot do not include heavy components and ball screws as part of the actuation process, which are usually included in wearable robots that make them uncomfortable for the user [53]. The real-time experiments, systematically performed to test the proposed layered architecture, showed that the wearable ankle–foot robot is capable of making accurate decisions, set the control signals for the next robot state and control the robot actions for the interaction and assistance to the human foot while walking. This proof-of-concept wearable ankle–foot robot has the potential to be used in different applications, for instance, to assist people during walking to reduce energy consumption, assist patients with foot-drop impairments, rehabilitation and telerobotics. The size of the wearable device might require to be updated for the specific person and application but the overall design and control approach remain the same. We are particularly interested in recruiting patients to evaluate the wearable ankle–foot system for assistance to foot-drop impairment, which is part of our future work plan.

Overall, this work offers an alternative methods for the reliable control of wearable robots that interact with the human body. This approach offers robust computational methods for accurate and fast recognition of walking and gait events. The wearable robot requires one IMU only, which optimises energy and weight. The control and recognition methods are implemented in an FPGA for fast data processing. The following limitations have been identified in the current version of the proposed human-in-the-loop layered architecture: adaptive decision-making to response to changing walking speeds, autonomous selection of decision threshold for the decision-making process, adaptive robot compliance through admittance control methods. These are the identified challenges and limitations that we plan to investigate and address in the future work.

6. Conclusion

This work presented a human-in-the-loop layered architecture for control of a wearable ankle–foot robot. This architecture composed of high-, mid- and low-level layers, interconnected and precisely synchronised, allowed the wearable robot to read data from sensors attached on the human body, make accurate decisions, set control parameters and control the robot actions to reliably interact with and assist the human foot while walking. The wearable robot employed to validate the layered architecture was developed using a 3D printing technology and a novel actuation system. The accuracy and precise control of the wearable robot, performed by the layered architecture, ensure a safe and reliable robot performance while interaction with the human body. For validation, experiments in simulation and real-time environments were systematically performed through the analysis of recognition accuracy for walking events and the control and response of the wearable robot while assisting the human foot. Overall, the experiments demonstrated that the proposed human-in-the-loop layered architecture is suitable for the development of smart wearable robots capable of safely interacting and assisting the human body.

Declaration of competing interest

The authors declare that they have no known competing financial interests or personal relationships that could have appeared to influence the work reported in this paper.

Data availability

Data will be made available on request.

Acknowledgements

This work was supported by the Engineering and Physical Sciences Research Council (EPSRC), UK for the 'Wearable soft robotics for independent living' project (EP/M026388/1) and the Royal Society, UK for the 'Touching and feeling the immersive world' project (RGS/R2/192346).

References

[1] A.T. Asbeck, S.M.M. De Rossi, I. Galiana, Y. Ding, C.J. Walsh, Stronger, smarter, softer: Next-generation wearable robots, Robot. Autom. Mag. IEEE 21 (4) (2014) 22–33.

[2] C. Rognon, S. Mintchev, F. Dell'Agnola, A. Cherpillod, D. Atienza, D. Floreano, Flyjacket: An upper body soft exoskeleton for immersive drone control, IEEE Robot. Autom. Lett. 3 (3) (2018) 2362–2369.

[3] U. Martinez-Hernandez, L.W. Boorman, T.J. Prescott, Multisensory wearable interface for immersion and telepresence in robotics, IEEE Sens. J. 17 (8) (2017) 2534–2541.

[4] Y. Mengüç, Y.-L. Park, H. Pei, D. Vogt, P.M. Aubin, E. Winchell, L. Fluke, L. Stirling, R.J. Wood, C.J. Walsh, Wearable soft sensing suit for human gait measurement, Int. J. Robot. Res. 33 (14) (2014) 1748–1764.

[5] E. Fullerton, B. Heller, M. Munoz-Organero, Recognising human activity in free-living using multiple body-worn accelerometers, IEEE Sens. J. 17 (16) (2017) 5290–5297.

[6] H. Huang, T.A. Kuiken, R.D. Lipschutz, A strategy for identifying locomotion modes using surface electromyography, IEEE Trans. Biomed. Eng. 56 (1) (2009) 65–73.

[7] R.A. Brooks, Intelligence without representation, Artificial Intelligence 47 (1–3) (1991) 139–159.

[8] L. Fraser, B. Rekabdar, M. Nicolescu, M. Nicolescu, D. Feil-Seifer, G. Bebis, A compact task representation for hierarchical robot control, in: 2016 IEEE-RAS 16th International Conference on Humanoid Robots (Humanoids), IEEE, 2016, pp. 697–704.

[9] T.J. Prescott, P. Redgrave, K. Gurney, Layered control architectures in robots and vertebrates, Adapt. Behav. 7 (1) (1999) 99–127.

[10] R. Simmons, T. Smith, M.B. Dias, D. Goldberg, D. Hershberger, A. Stentz, R. Zlot, A layered architecture for coordination of mobile robots, in: Multi-Robot Systems: From Swarms to Intelligent Automata, Springer, 2002, pp. 103–112.

[11] A. De Santis, B. Siciliano, A. De Luca, A. Bicchi, An atlas of physical human–robot interaction, Mech. Mach. Theory 43 (3) (2008) 253–270.

[12] R.A. Brooks, A robust layered control system for a mobile robot, IEEE J. Robot. Autom. 2 (1) (1986) 14–23.

[13] S. Thrun, W. Burgard, D. Fox, Probabilistic Robotics, MIT Press, 2005.

[14] U. Martinez-Hernandez, I. Mahmood, A.A. Dehghani-Sanij, Simultaneous Bayesian recognition of locomotion and gait phases with wearable sensors, IEEE Sens. J. 18 (3) (2018) 1282–1290, http://dx.doi.org/10.1109/JSEN.2017.2782181.

[15] U. Martinez-Hernandez, A. Rubio-Solis, V. Cedeno-Campos, A.A. Dehghani-Sanij, Towards an intelligent wearable ankle robot for assistance to foot drop, in: 2019 IEEE International Conference on Systems, Man and Cybernetics (SMC), IEEE, 2019, pp. 3410–3415.

[16] V. Rajasekaran, J. Aranda, A. Casals, J.L. Pons, An adaptive control strategy for postural stability using a wearable robot, Robot. Auton. Syst. 73 (2015) 16–23.

[17] D. Novak, R. Riener, A survey of sensor fusion methods in wearable robotics, Robot. Auton. Syst. 73 (2015) 155–170.

[18] J.L. Pons, Wearable Robots: Biomechatronic Exoskeletons, John Wiley & Sons, 2008.

[19] L. Peeraer, B. Aeyels, G. Van der Perre, Development of EMG-based mode and intent recognition algorithms for a computer-controlled above-knee prosthesis, J. Biomed. Eng. 12 (3) (1990) 178–182.

[20] H. Kawamoto, Y. Sankai, Comfortable power assist control method for walking aid by HAL-3, in: Systems, Man and Cybernetics, 2002 IEEE International Conference on, 4, IEEE, 2002, pp. 6–pp.

[21] J. Staudenmayer, D. Pober, S. Crouter, D. Bassett, P. Freedson, An artificial neural network to estimate physical activity energy expenditure and identify physical activity type from an accelerometer, J. Appl. Physiol. 107 (4) (2009) 1300–1307.

[22] A.M. Khan, Y.-K. Lee, T.-S. Kim, Accelerometer signal-based human activity recognition using augmented autoregressive model coefficients and artificial neural nets, in: Engineering in Medicine and Biology Society, 2008. EMBS 2008. 30th Annual International Conference of the IEEE, IEEE, 2008, pp. 5172–5175.

[23] K. Yuan, A. Parri, T. Yan, L. Wang, M. Munih, Q. Wang, N. Vitiello, A realtime locomotion mode recognition method for an active pelvis orthosis, in: Intelligent Robots and Systems (IROS), 2015 IEEE/RSJ International Conference on, IEEE, 2015, pp. 6196–6201.

[24] S.E. Hussein, M.H. Granat, Intention detection using a neuro-fuzzy EMG classifier, Eng. Med. Biol. Mag. IEEE 21 (6) (2002) 123–129.

[25] H. Huang, F. Zhang, L.J. Hargrove, Z. Dou, D.R. Rogers, K.B. Englehart, Continuous locomotion-mode identification for prosthetic legs based on neuromuscular–mechanical fusion, IEEE Trans. Biomed. Eng. 58 (10) (2011) 2867–2875.

[26] J. Wannenburg, R. Malekian, Physical activity recognition from smartphone accelerometer data for user context awareness sensing, IEEE Trans. Syst. Man Cybern.: Syst. 47 (12) (2016) 3142–3149.

[27] U. Martinez-Hernandez, T.J. Dodd, T.J. Prescott, Feeling the shape: Active exploration behaviors for object recognition with a robotic hand, IEEE Trans. Syst. Man Cybern.: Syst. 48 (12) (2018) 2339–2348, http://dx.doi.org/10.1109/TSMC.2017.2732952.

[28] U. Martinez-Hernandez, T.J. Dodd, M.H. Evans, T.J. Prescott, N.F. Lepora, Active sensorimotor control for tactile exploration, Robot. Auton. Syst. 87 (2017) 15–27.

[29] J. Ferreira, J. Lobo, P. Bessiere, M. Castelo-Branco, J. Dias, A Bayesian framework for active artificial perception, IEEE Trans. Cybern. 43 (2) (2013) 699–711.

[30] S. Mohammed, A. Same, L. Oukhellou, K. Kong, W. Huo, Y. Amirat, Recognition of gait cycle phases using wearable sensors, Robot. Auton. Syst. 75 (2016) 50–59.

[31] A.J. Young, A.M. Simon, N.P. Fey, L.J. Hargrove, Intent recognition in a powered lower limb prosthesis using time history information, Ann. Biomed. Eng. 42 (3) (2014) 631–641.

[32] H.A. Varol, F. Sup, M. Goldfarb, Multiclass real-time intent recognition of a powered lower limb prosthesis, IEEE Trans. Biomed. Eng. 57 (3) (2010) 542–551.

[33] F.R. Allen, E. Ambikairajah, N.H. Lovell, B.G. Celler, Classification of a known sequence of motions and postures from accelerometry data using adapted Gaussian mixture models, Physiol. Meas. 27 (10) (2006) 935.

[34] X. Liu, Z. Zhou, J. Mai, Q. Wang, Real-time mode recognition based assistive torque control of bionic knee exoskeleton for sit-to-stand and stand-to-sit transitions, Robot. Auton. Syst. 119 (2019) 209–220.

[35] A.T. Asbeck, K. Schmidt, C.J. Walsh, Soft exosuit for hip assistance, Robot. Auton. Syst. 73 (2015) 102–110.

[36] D.Y. Li, A. Becker, K.A. Shorter, T. Bretl, E.T. Hsiao-Wecksler, Estimating system state during human walking with a powered ankle-foot orthosis, IEEE/ASME Trans. Mechatronics 16 (5) (2011) 835–844.

[37] P.K. Jamwal, S.Q. Xie, S. Hussain, J.G. Parsons, An adaptive wearable parallel robot for the treatment of ankle injuries, IEEE/ASME Trans. Mechatronics 19 (1) (2014) 64–75.

[38] J.A. Saglia, N.G. Tsagarakis, J.S. Dai, D.G. Caldwell, Control strategies for patient-assisted training using the ankle rehabilitation robot (ARBOT), IEEE/ASME Trans. Mechatronics 18 (6) (2013) 1799–1808.

[39] D. Rus, M.T. Tolley, Design, fabrication and control of soft robots, Nature 521 (7553) (2015) 467.

[40] Y.-L. Park, J. Santos, K.G. Galloway, E.C. Goldfield, R.J. Wood, A soft wearable robotic device for active knee motions using flat pneumatic artificial muscles, in: Robotics and Automation (ICRA), 2014 IEEE International Conference on, IEEE, 2014, pp. 4805–4810.

[41] P. Polygerinos, Z. Wang, K.C. Galloway, R.J. Wood, C.J. Walsh, Soft robotic glove for combined assistance and at-home rehabilitation, Robot. Auton. Syst. 73 (2015) 135–143.

[42] C. Zhu, W. Sheng, Wearable sensor-based hand gesture and daily activity recognition for robot-assisted living, IEEE Trans. Syst. Man Cybern.- A: Syst. Hum. 41 (3) (2011) 569–573.

[43] A.J. Young, L.J. Hargrove, A classification method for user-independent intent recognition for transfemoral amputees using powered lower limb prostheses, IEEE Trans. Neural Syst. Rehabil. Eng. 24 (2) (2015) 217–225.

[44] S. Kyeong, W. Shin, M. Yang, U. Heo, J.-r. Feng, J. Kim, Recognition of walking environments and gait period by surface electromyography, Front. Inf. Technol. Electron. Eng. 20 (3) (2019) 342–352.

[45] S. Potluri, A.B. Chandran, C. Diedrich, L. Schega, Machine learning based human gait segmentation with wearable sensor platform, in: 2019 41st Annual International Conference of the IEEE Engineering in Medicine and Biology Society (EMBC), IEEE, 2019, pp. 588–594.

[46] A. Rattanasak, P. Uthansakul, M. Uthansakul, T. Jumphoo, K. Phapatanaburi, B. Sindhupakorn, S. Rooppakhun, Real-time gait phase detection using wearable sensors for transtibial prosthesis based on a kNN algorithm, Sensors 22 (11) (2022) 4242.

[47] F. Sherratt, A. Plummer, P. Iravani, Understanding LSTM network behaviour of IMU-based locomotion mode recognition for applications in prostheses and wearables, Sensors 21 (4) (2021) 1264.

[48] S.K. Challa, A. Kumar, V.B. Semwal, A multibranch CNN-BiLSTM model for human activity recognition using wearable sensor data, Vis. Comput. (2021) 1–15.

[49] J. Zeni Jr., J. Richards, J. Higginson, Two simple methods for determining gait events during treadmill and overground walking using kinematic data, Gait Post. 27 (4) (2008) 710–714.

[50] M.R. Tucker, J. Olivier, A. Pagel, H. Bleuler, M. Bouri, O. Lambercy, J. del R Millán, R. Riener, H. Vallery, R. Gassert, Control strategies for active lower extremity prosthetics and orthotics: a review, J. Neuroeng. Rehabil. 12 (1) (2015) 1.

[51] Y.-L. Park, B.-r. Chen, D. Young, L. Stirling, R.J. Wood, E.C. Goldfield, R. Nagpal, et al., Design and control of a bio-inspired soft wearable robotic device for ankle-foot rehabilitation, Bioinspiration Biomim. 9 (1) (2014) 016007.

[52] K.A. Shorter, G.F. Kogler, E. Loth, W.K. Durfee, E.T. Hsiao-Wecksler, A portable powered ankle-foot orthosis for rehabilitation, J. Rehabil. Res. Dev. 48 (4) (2011).
[53] D.P. Ferris, K.E. Gordon, G.S. Sawicki, A. Peethambaran, An improved powered ankle–foot orthosis using proportional myoelectric control, Gait Posture 23 (4) (2006) 425–428.

Uriel Martinez-Hernandez received the B.Eng. degree in Communications and Electronics from the National Polytechnic Institute, Mexico, in 2005. He obtained the M.Sc. degree in Computer Science from the Centre for Research and Advanced Studies, Mexico, in 2008. He received the Ph.D. degree from the Department of Automatic Control and Systems Engineering, University of Sheffield, Sheffield, U.K., in 2015. He was a Research Associate and Research Fellow at Sheffield Robotics, the University of Sheffield and the School of Mechanical Engineering, the University of Leeds, respectively. He is currently a Lecturer (Assistant Professor) in Robotics and Autonomous Systems at the Department of Electronics and Electrical Engineering, and the Centre for Autonomous Robotics (CENTAUR), University of Bath, U.K. His research interests include active sensing and perception with touch and vision, wearable assistive robotics, machine learning for autonomous robots and human–robot interaction.

Sina Firouzy received his Ph.D. degree from the Department of Mechanical Engineering at the University of Leeds, UK, in 2018. He is currently a Research Fellow in Robotics at the University of Portsmouth, UK. His research interests include dynamic analysis and simulation, design and control in Robotics.

Pouyan Mehryar obtained his Master of Engineering (M.Eng.) with first-class honours in Mechanical and Medical Engineering from the University of Hull. He received his Ph.D. degree from the institute of Design, Robotics and Optimisation (iDRO), School of Mechanical Engineering at the University of Leeds, UK, in 2018. After obtaining his Ph.D., He was a Postdoctoral Research Fellow and appointed as a postdoctoral Teaching Fellow at the School of Mechanical Engineering, the University of Leeds. He is currently a Postdoctoral Researcher at the Healthcare Innovation Centre of the Teesside University based in The Welding Institute, Cambridge, UK. His research interests lie in the areas of biomechanics, clinical movement analysis, rehabilitation robotics, artificial intelligence, multibody dynamics, tissue engineering and regenerative medicine.

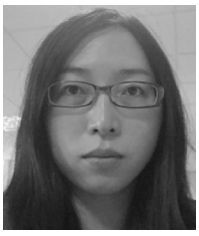

Lin Meng received the Ph.D. degree from the division of Biomedical Engineering, University of Glasgow, Glasgow, U.K., in 2016. She is currently an Associate professor at Tianjin International Joint Research Center for Neural Engineering, Academy of Medical Engineering and Translational Medicine, Tianjin University, Tianjin, China. Her research interests include motion analysis, wearable sensing technologies and assistive robotics.

Craig Childs received the Ph.D. degree from the University of Aalborg, Denmark. He is currently a Research Fellow at the Biomedical Engineering Department at the University of Strathclyde, Glasgow, UK. He is a Clinical Scientist registered with the HCPC. His research interests include motion analysis, gait stability, virtual reality feedback, wearable sensors and accessibility.

Arjan Buis received the Ph.D. degree from the University of Strathclyde. He is currently an Associate professor at the Biomedical Engineering department at the University of Strathclyde, Glasgow, UK. He is a biomedical engineer and Sr, prosthetist & Orthotist. His research interests include the body device interface, wearable sensing technologies and assistive robotics. He has published over 100 journal and conference papers.

Abbas A. Dehghani-Sanij received the Ph.D. degree from the University of Leeds, Leeds, U.K. He is currently Professor of Bio-Mechatronics and Medical Robotics in the School of Mechanical Engineering at the University of Leeds. His research interests include robotics, biomechatronics, intelligent control, sensors and actuators for the development of intelligent systems/devices. He has published more than 150 journal and conference papers.